

Adaptive Beam Forming of MIMO System using Low Complex Selection of Steering Vector

¹P. Sekhar Babu, ²P.V. Naganjaneyulub and ¹K. Satya Prasad
¹Department of Electronics and Communication Engineering,
Jawaharlal Nehru Technological University, Kankinada, India
²Department of Electronics and Communication Engineering,
M.V.R College of Engineering and Technology, Vijayawada, India

Abstract: With the superior growth of digital communication the need for high-speed data transmission has increased. In that Orthogonal Frequency Division Multiplexing (OFDM) is a multi-carrier modulation technique which partition the single spectrum into numerous sub-carriers. The major benefit of OFDM is their significance towards channel fading in wireless environment. In wide range data transmission, the OFDM is heavily affected by the Inter Symbol Interface (ISI). To diminish ISI an Adaptive Analog Beam Forming (AABF) based Phased Array Antenna (PAA) is introduced. PAA achieves the reduction of noise significantly and also shows improvement in the effectiveness of reducing the side lobe ranges with narrow beam width. The experimental outcome proves that the proposed system performs effectively than the other existing systems.

Key words: Adaptive analog beam forming, orthogonal frequency division multiplexing, phased array antenna, channel state information, inter symbol interface, narrow beam

INTRODUCTION

In the past few decades, there have been intensive research in developing effective multiuser transmission methods for wireless system (Serbetli and Yener, 2004). Multi Users-OFDM (MU-OFDM) has become an emerging technique in 4 and 5th generation wireless communication (Luo *et al.*, 2013; Yang and Yue, 2015). The MU technology transmits numerous signal over several antennas and OFDM partition the single radio signal into equally spaced sub-signals to deliver less distortion rate at high speed broadcast (Shrivastava and Trivedi, 2015). The major issue in wireless communication is ISI, several techniques are implemented to decrease ISI (Eisenberg and Tabrikian, 2013). In that Beam Forming (BF) can effectively improve the reliability of transmission and also achieve high data rate (Hung and Tsai, 2014). Generally, BF is performed on the basis of analog and digital. In this research, the analog BF is preferred for implementation as it improves the performance of target orientation. Initially, BF was implemented in unipolar and bipolar antennas to increase the signal capacity and also for improving the signal strength.

Still, BF requires Channel State Information (CSI), because it helps to denote the channel property of communication link and also to avoid complex

equalization at the receiver. Hence, the Rayleigh channel is preferred for CSI. Practically, suitable CSI is not obtainable at the transmitter system and the impact of quantized or noisy CSI is very excessive (Kim *et al.*, 2011). To enhance the spatial diversity gain or to reduce the cross correlation of the signals reflected back to the antenna by the target of interest, a flexible system was designed named Phased Array Antenna (PAA). It has the capacity to direct the beam pattern electronically with extraordinary effectiveness and also it manages to get minimal side lobe level with narrow beam width (Ruan and Lamare, 2014). To achieve scanning range with high angle resolution an enormous number of antenna components are required to implement the array. Usage of the microwave components in an enormous quantity may cause frequent obstacles in limited coverage areas and also it gets complex during deformation. So, to overcome these concerns a traditional PAA is improved as adaptive PAA which enhance the antenna gain and improves the directivity of the main lobe.

Literature review: Hassanien and Vorobyov (2010) have illustrated a phased-Multiple-Input Multiple-Output (MIMO) radar which was the grouping of both MIMO radar and colocated antennas. Initially, the transmit array was sub-divided into a number of sub-arrays that were

permitted to overlap. In each sub-array, coherent processing was attained by employing a weight vector scheme. Simulation outcome determines, phased MIMO radar shows a superior result in Signal to Interference plus Noise Ratio (SINR) compared to phased array and MIMO radar techniques.

Wang (2013) have developed a phased MIMO radar with range dependent BF method for frequency diversity. The essence of this system was to partition the frequency diverse transmit array into numerous sub-arrays. Each sub-array beams were independently steerable by tuning the frequency increment. Sub-arrays delivered an effective operating modes and range-dependent BF which was surveyed by examining the transmit-receive beam-patterns and the output SINR. The effectiveness of this technique was verified by the developers in their numerical simulation results. They concluded by describing that another potential future work is the application of phased MIMO radar.

Deligiannis *et al.* (2014) have presented a transmit BF scheme for 2 Dimensional (2D) phased MIMO radar. In this research, sub-aperturing technique for 2D transmit arrays with in the context of MIMO radar was examined. To attain high coherent processing gain, a weight vector should be designed for each sub-array to steer the transmit beam in a certain 2D sector which diminishes the variation between desired transmit and actual beam pattern. The actual beam pattern was formed by 2D array of antennas, under a constraint of uniform power allocation across the transmit antennas.

Jiang *et al.* (2014) presented a scheme to form narrower main lobe of virtual transmitting-receiving BF by transmitting orthogonal coding waveforms from the antenna elements and digitally processing of their echoes at the receiver. With the help of amplitude taper method, a narrower main beam was attained with dense array configuration which enhance the slow moving target detection performance. The Signal to Noise Ratio (SNR) loss of tapering was also reviewed in this research.

MATERIALS AND METHODS

This study evaluates the directivity of the antenna that is enhanced by adaptive PAA by reducing the side lobes and also by decreasing the antenna components. Generally, the radio signals are spread out in all directions by a distinct antenna and similarly, a distinct antenna will collect signals evenly from all directions. Assume, a linear antenna array sensors and K narrow band signals received at i-th snapshot as expressed by:

$$x(i) = V(\theta)s(i)+n(i) \tag{1}$$

Where:

- $\theta = (\theta_1, \theta_2, \dots, \theta_k)^T \subseteq R^k$ = The vector containing the Directions of Arrival (DoAs)
- $s(i) \in C^{K \times 1}$ = The uncorrelated source signal
- $V(\theta)$ = The matrix containing Steering Vector (SV) which is denoted as $V(\theta) = [v(\theta_1)+e, \dots, v(\theta_k)] \subseteq C^{M \times K}$
- e = The SV for the mismatched signals
- $n(i)$ = Specified as zero mean and variance of Gaussian noise

Hence, AABF can point beam in many direction and manipulate beam shape to enhance system performance by varying the Vector $V(\theta)$.

Analog beamforming: It is expensive to insert a complete RF receiver chain and high-rate high-resolution analog channels unit for each antenna. Thus, let consider an Analog Pre-processing Network (APN) inserted in RF domain immediately after the low-noise amplifiers and bandpass filter. The effect of APN on the baseband signal is modeled using a discrete time equivalent matrix operation. Consider a linear BF signal with the output given by:

$$y(i) = w^H x(i) \tag{2}$$

Where:

- $w [w_1, \dots, w_M]^T \in C^{K \times 1}$ = The beam-former weight vector
- H = The Hermitian transpose

Optimum beam-former can be computed by maximizing the SINR which is given by:

$$SINR = \frac{\sigma_1^2 |w^H a|^2}{w^H R_{i+n} w} \tag{3}$$

where, summarized SV is stated as α and the Desired Signal Power (DSP) is mentioned as σ_1^2 , INC matrix is mentioned as R_{i+n} . Then, the issue in Eq. 3 can be converted into an optimization issue which is generally named as MVDR beam-former or Capon beam-former:

$$\begin{aligned} & \text{Minimize } w^H R_{i+n} w \\ & \text{Subject to } w^H a = 1 \end{aligned} \tag{4}$$

The INC matrix is found by determining the Sample Covariance Matrix (SCM) of the received data as:

$$\hat{R}(i) = \frac{1}{i} \sum_{k=1}^i x(k)x^H(k) \tag{5}$$

Implementation of Phased Array Antenna (PAA): The PAA is composed by similar group antennas, each antenna consists of summing network, phase shifter, power feed network and that helps to represent a beam on a desired location. In RF stage, the analog components like low noise and power amplifiers are required to condition the both transmitted and received signals in antenna array. Incident plane wave of antenna receiver can be demonstrated by following equation:

$$f(t, p_n) = C_n(t) = x(t - \tau_n) \cos(w_{RF}(t - \tau_n)) \quad (6)$$

$$n = 0, \dots, N-1$$

$$\approx x(t) \cos(w_{RF}t - \theta_n) \quad (7)$$

where, θ_n is given by:

$$\theta_n = w_{RF}\tau \quad (8)$$

After that the respective incoming signals reaches RF modulation stage. Here, the frequency components of incoming signals are associated to ADCs and analog signal modulation is needed to shift the signal's frequency components into a lower frequency band. If the RF stage has local oscillator with a frequency of w_{LO} , then the modulated beam from PAA can be termed in the following form:

$$g_n(t) = x(t) \cos(w_{RF}t - \theta_n) \cos(w_{LO}(t)) \quad (9)$$

where, k is modulated as time signal t , analog beam $y(i)$ is replaced by the PAA's analog beam $g_n(t)$.

Estimation of Steering Vector (SV) using proposed PAA analog beam: The cross-correlation relationship between the array observation vector and the beam-former output can be specified as follows:

$$d = E \{ x g_n \} \quad (10)$$

where, the vector v is considered as $|v_m^H w| \ll |v_1^H w|$ for $m = 2, \dots, K$. Hence, all the source and noise signals have zero mean, substitute the Eq. 1 and 9 in Eq. 10 which is mathematically stated as:

$$d = E \{ \sigma_1^2 v_1^H w w_1 + t w \} \quad (11)$$

In which the unwanted interference that cause noise and signal power loss are eliminated. Then, the SV is projected into the sub-space and the projection matrix P is calculated as:

$$P = [c_1, c_2, \dots, c_p] [c_1, c_2, \dots, c_p]^H \quad (12)$$

where, c_1, c_2, \dots, c_p are the p Eigen vectors from the vector of matrix C which is given as:

$$C = \int_{\theta_1 - \theta_s}^{\theta_1 + \theta_s} v(\theta) v^H(\theta) d\theta \quad (13)$$

Oracle Approximating Shrinkage (OAS) technique is utilized by the PAA method to evaluate the correlation vector. An accurate estimation helps to achieve a better estimate of SV. It can be specified as:

$$\hat{F} = \hat{r} I \quad (14)$$

Where:

$$\hat{r} = \text{tr}(\hat{S})/S \text{ and } \hat{S} = \text{diag}(x g_n)$$

A reasonable trade-off between reduction in covariance and bias growth can be attained by shrinkage of \hat{S} and \hat{F} results are:

$$\hat{d} = \hat{\rho} \text{diag}(\hat{F}) + (1 - \hat{\rho}) \text{diag}(\hat{S}) \quad (15)$$

Which is parameterized by the shrinkage co-efficient $\hat{\rho}$, utilized for reducing the Mean Square Error (MSE) and the Sample Correlation Vector (SCV) is specified in Eq. 16 as:

$$\hat{S}(i) = \text{diag} \left(\frac{1}{i} \sum_{k=1}^i x(k) g_n(k) \right) \quad (16)$$

Once, the correlation vector is attained by the above OAS technique, the SV is estimated by:

$$\hat{a}_1(i) = \frac{P \hat{d}(i)}{\|P \hat{d}(i)\|_2} \quad (17)$$

where, $\hat{a}_1(i)$ gives the final estimate of SV and by identifying the SV, beam formed by the PAA is estimated. Thus, the PAA implementation and the SV are identified for the analog signals and the adaptive analog beam-former is detected:

$$\hat{d}(i) = \hat{\rho}(i) \text{diag}(\hat{F}(i)) + (1 - \hat{\rho}(i)) \text{diag}(\hat{S}(i)) \quad (18)$$

$$\hat{\rho}(i+1) = \frac{\left(1 - \frac{2}{M}\right) \text{tr}(\hat{D}(i) \hat{S}^*(i))}{\left(i + 1 - \frac{2}{M}\right) \text{tr}(\hat{D}(i) \hat{S}^*(i))} + \frac{\text{tr}(\hat{D}(i)) \text{tr}(\hat{D}^*(i))}{\left(1 - \frac{i}{M}\right) \text{tr}(\hat{D}(i)) \text{tr}(\hat{D}^*(i))} \quad (19)$$

Interference Plus-Noise Covariance Matrix (IP-NCM)

determination: To evaluate INC matrix, the data covariance matrix is required and the SCM in Eq. 5 is essential as an initial approximation. In the next step, similar to OAS estimate, the cross-correlation vector d is performed with OAS technique for further shrinkage determination step. It is defined as:

$$\hat{F}_0 = \hat{v}_0 I \tag{20}$$

where, $\hat{v}_0 = \text{tr}\hat{R}/M$ and utilize the shrinkage form again:

$$\hat{R} = \hat{p}_0 \hat{F}_0 + (1-\hat{p}_0) \hat{R} \tag{21}$$

By reducing the MSE which is termed as $E\|\hat{R}(i)-\hat{F}_0(i-1)\|^2$ then obtain the following recursion:

$$\hat{R}(i) = \hat{p}_0(i) \hat{F}_0(i) + (1-\hat{p}_0(i)) \hat{R}(i) \tag{22}$$

$$\hat{p}_0(i+1) = \frac{\left(1-\frac{2}{M}\right) \text{tr}(\hat{R}(i) \hat{R}(i))}{\left(i+1-\frac{2}{M}\right) \text{tr}(\hat{R}(i) \hat{R}(i))} + \frac{\text{tr}^2(\hat{R}(i))}{\left(1-\frac{i}{M}\right) \text{tr}^2(\hat{R}(i))} \tag{23}$$

Provided that $0 < \hat{p}_0(0) < 1$, the iterative progression in Eq. 22 and 23 is guaranteed to converge Eq. 18. To eradicate the un-wanted information of desired signal in the covariance and INC matrix, the DSP σ_1^2 must be estimated. Received data can be modified as:

$$x = \sum_{k=1}^k a(k) s(k) + n \tag{24}$$

Pre-multiplying the Eq. 24 by a_1^H which is illustrated as:

$$a_1^H x = a_1^H a_1 s_1 + a_1^H \left(\sum_{k=1}^k a(k) s(k) + n \right) \tag{25}$$

Considering that a_1 is un-correlated with the interferers, Eq. 25 is updated as:

$$a_1^H x = a_1^H a_1 s_1 + a_1^H n \tag{26}$$

Assuming the expectation of $E\|(a_1^H x)^2\|$ where Eq. 26 is expanded as follows:

$$(a_1^H x)^2 = E\left[(a_1^H a_1 s_1 + a_1^H n) \times (a_1^H a_1 s_1 + a_1^H n) \right] \tag{27}$$

If the noise is independent of the desired signal and it is mathematically stated as:

$$(a_1^H x)^2 = (a_1^H a_1)^2 (s_1)^2 + a_1^H n n^H a_1 \tag{28}$$

where, $(s_1)^2$ is the DSP which is inter-changed by its estimate $\hat{\sigma}_1^2$ and $n n^H$ is represented as NCM R_n which is inter-changed by $\sigma_1^2 I_M$. Replacing, the general estimate a_1 as DSP estimate $\hat{a}_1(i)$ which is demonstrated as:

$$\lambda = \frac{2(\hat{\sigma}_1^2(i) \hat{a}_1^H(i) \hat{a}_1(i) - g(i) x^H(i) \hat{a}_1(i))}{\hat{a}_1^H(i) \hat{a}_1(i)} \tag{29}$$

Finally, the desired signal of covariance matrix is subtracted and the INC matrix is stated by:

$$\hat{R}_{i+n}(i) = \lambda \hat{R}(i) - \hat{\sigma}_1^2(i) \hat{a}_1(i) \hat{\sigma}_1^H(i) \tag{30}$$

where, λ is deliberated as a weight function. In AABF scheme, a weight function is employed for minimizing the BER. Usually, BER is inversely associated with the quality of signals. Once, the BER is minimized means, the quality of the signals get improved:

$$\hat{\sigma}_1^2 = \frac{|\hat{a}_1^H(i) x_1(i)|^2 - \hat{a}_1^H(i) \hat{a}_1(i) \hat{\sigma}_n^2}{|\hat{a}_1^H(i) a_1(i)|^2} \tag{31}$$

The benefit of this step compared to SMI and existing approaches, it does not need direction finding. With the estimates for the SV and the INC matrix, the beam-former is computed by:

$$\hat{w}(i) = \frac{\hat{R}_{i+n}^{-1}(i) \hat{a}_1(i)}{\hat{a}_1^H(i) \hat{R}_{i+n}^{-1}(i) \hat{a}_1(i)} \tag{32}$$

RESULTS AND DISCUSSION

Simulation and analysis of the outcome is done by employing Uniform Linear Array (ULA) $M = 12$ with a space of half wavelength. Initially, three source signals are added to the desired signal, the first one is recognized at $\theta_1 = 10^\circ$ and the remaining two interferers are interrupting on the antenna array from the directions $\theta_2 = 50^\circ$ and $\theta_3 = 90^\circ$. The Signal to Interference Ratio (SIR) is fixed at 20 dB. Only one iteration is achieved per snapshot and employ $i = 50$ snapshots and 100 repetitions to obtain each point of the curves.

The beam-former computed with Low Complexity Shrinkage based Mismatch Estimation algorithm (LOCSME) is compared to existing beam-formers in terms of output SINR. For the beam-formers of LOCSME, inverse LOCSME and the proposed scheme of AABF on phased antenna, the angular section is chosen as $[\theta_1-5^\circ, \theta_2+5^\circ]$ and $p = 8$ principal eigenvectors are used. Eigenvectors of the subspace projection matrix p is selected manually with the help of simulation.

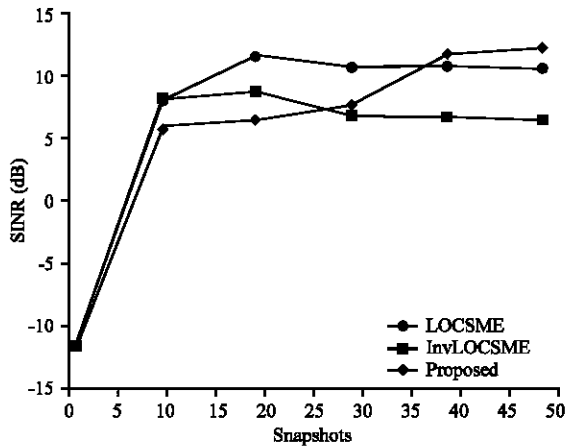


Fig. 1: SINR vs. snapshot

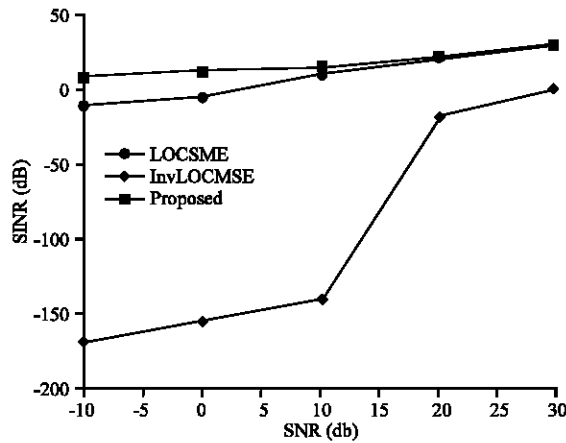


Fig. 2: SINR vs. SNR

For the beam-formers of LOCSME, inverse LOCSME and the proposed approach which requires an optimization technique, the MATLAB CVX Software is employed. Algorithms (SINR vs. snapshot and SINR vs. SNR) performance are shown in Fig. 1 and 2. In Fig. 1, the existing schemes LOCSME and inverse LOCSME shows 11 and 6 dB, respectively. Compared to these two schemes, the proposed performance proves with a significant outcome of 12 dB. The AABF technique confirms that the number of snapshots increases means the SINR value is also improved.

In Fig. 2, SINR performance of the existing two methods and the proposed system (AABF) is signified in a graphical form. The number of snapshot is 50 for (SINR vs. SNR) plots and the regular execution time of the algorithms in the early methods are around 0.3 sec/snapshot where the proposed scheme requires only 0.016 sec/snapshot.

In Fig. 3, BER performance of the existing two methods and the proposed approach is denoted in a

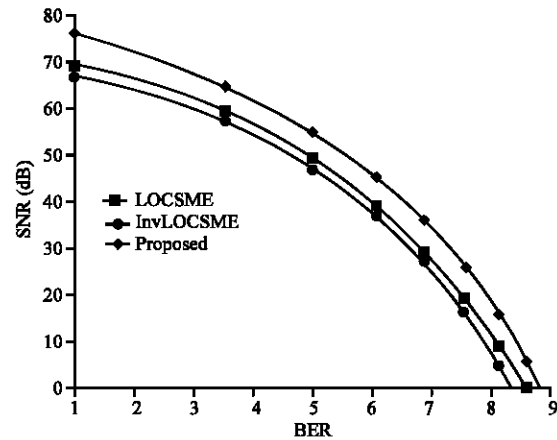


Fig. 3: BER vs. SNR

graphical form. It specifies that the performance of proposed approach (AABF is -11 dB) is superior in terms of SNR:

$$SNR (dB) = 10 \log \left(\frac{\hat{p} \text{ signal}}{\hat{p} \text{ noise}} \right) \quad (33)$$

Usually, OFDM converts the multi-path channel into N fading channel. Then, derive the BER equation over Rayleigh channels $P_b(E)$. General equation for BER is specified as:

$$BER = \frac{1}{N} \sum_{K=1}^N P_b, K(E) \quad (34)$$

where, K is demonstrated as sub-carrier index. Following graph determines the cumulative outcome because it varies based on the number of snapshots utilized.

Mismatch due to Coherent Local Scattering (CLS):

Figure 1 and 2 illustrate (SINR vs. snapshot and SINR vs. SNR) performance under CLS case. The proposed AABF method out-performs the other algorithms which is near to the optimal SINR.

Mismatch due to Incoherent Local Scattering (ILS):

Figure 1 and 2 depicts (SINR vs. snapshot and SINR vs. SNR) performance. Compared to CLS, all the algorithms have performance reduction due to ILS effect. However, the proposed methodology is able to out-perform the remaining robust beam-formers over an extensive range of input SNR. The reason for the improved performance of proposed scheme is the combination of INC matrix and SV mismatch in array antenna. Further, testing with a higher number of antenna array elements specifies that the performance of all algorithms degrades (e.g., AABF in PAA) has around 2 dB degradation when $M = 60$. In addition, inappropriate choice of angular sector also leads to noticeable performance degradation.

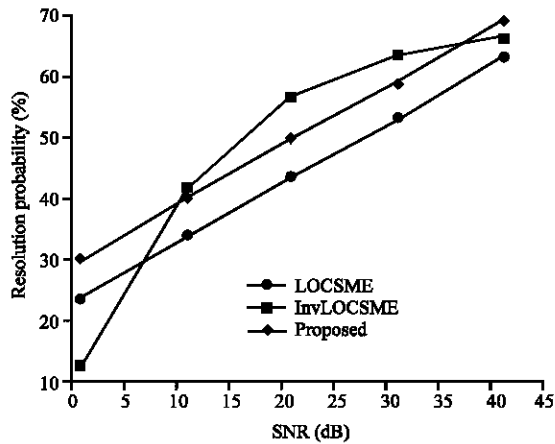


Fig. 4: Resolution probability vs. SNR

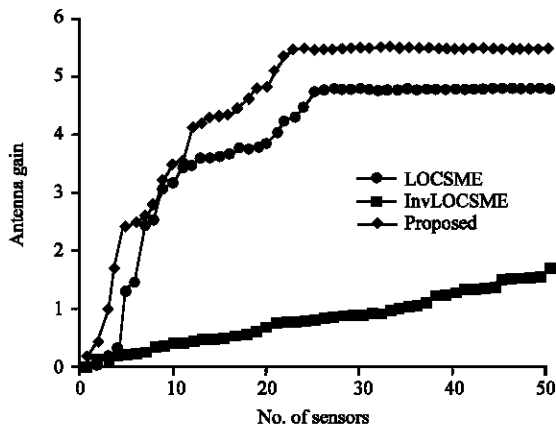


Fig. 5: Antenna gain vs. No. of sensors

Figure 4 specifies the enactment evaluation of proposed and existing approaches in terms of resolution probability. It clearly shows that the proposed scheme delivers 69.90% of resolution probability which is 4.40 and 7.90% more than the existing approaches inverse LOCSME and LOCSME. From the Fig. 4, the proposed method and LOCSME shows linear in variation but the inverse-LOCSME scheme delivers random variation that is due to random sequence generation. Here, the number of sensor undertaken is 12 and the number of interference is 10.

Figure 5 determines the antenna gain in terms of sensors, number of sensors undertaken 12. In this research, number of interference and snapshots utilized for experimental analysis are 3 and 50, respectively. Figure 5 clearly shows that the proposed scheme outperforms existing approaches. Whereas, the proposed method gives 5.41 dB antenna gain and the existing schemes shows 4.87 and 1.76 dB gain. Hence, the peak gain for dipole antenna is 7.85 dB. This proposed method almost achieved a better antenna gain only with a difference of 2.44 dB in comparison with ideal antenna.

CONCLUSION

This study presents a simple, effective adaptive BF algorithm which is robust against covariance matrix uncertainty. In MU-OFDM, the concern of ISI is continually affecting the signal transmission performance by creating numerous noise, distortion and variations in the BF signals. Here, (SINR vs. snapshot and SINR vs. SNR) performance is evaluated and shown as a graphical representation. Simulation result confirms that the proposed PAA out-performs in an efficient manner in the both ranges of CLS and ILS cases.

RECOMMENDATION

Further, testing with a higher number of antenna array elements specifies that the performance of proposed PAA is considerably significant than the previous approaches.

REFERENCES

- Deligiannis, A., J.A. Chambers and S. Lambouharan, 2014. Transmit beamforming design for two-dimensional phased-MIMO radar with fully-overlapped subarrays. Proceedings of the International Conference on Sensor Signal Processing for Defence (SSPD), September 8-9, 2014, IEEE, Edinburgh, UK., ISBN:978-1-4799-5294-6, pp: 1-4.
- Eisenberg, Y. and J. Tabrikian, 2013. Low complexity bit and power allocation for MIMO-OFDM systems using space-frequency beamforming. Signal Process., 93: 1961-1975.
- Hassanien, A. and S.A. Vorobyov, 2010. Phased-MIMO radar: A tradeoff between phased-array and MIMO radars. IEEE. Trans. Signal Process., 58: 3137-3151.
- Hung, Y.C. and S.H. Tsai, 2014. PAPR analysis and mitigation algorithms for beamforming MIMO OFDM systems. IEEE. Trans. Wireless Commun., 13: 2588-2600.
- Jiang, Y., W. Zhang, H. Li and C. Luo, 2014. Virtual Transmitting-Receiving Beamforming Approach to Achieving Narrower Mainlobe for MIMO Radar by Tapering. In: Signal Processing and Systems, Zhang, B., J. Mu, W. Wang, Q. Liang and Y. Pi (Eds.), Springer, Berlin, Germany, ISBN:978-3-319-00535-5, pp: 525-532.
- Kim, K., K. Ko and J. Lee, 2011. Adaptive selection of antenna grouping and beamforming for MIMO systems. EURASIP. J. Wireless Commun. Networking, Vol. 2011,
- Luo, W., A. Guo, W. Tan and Y. Ji, 2013. An improved beamforming method based on SLNR for downlink multi-user multi-stream MIMO system. Wireless Pers. Commun., 72: 2673-2683.

- Ruan, H. and D.R.C. Lamare, 2014. Robust adaptive beamforming using a low complexity shrinkage based mismatch estimation algorithm. *IEEE. Signal Process. Lett.*, 21: 60-64.
- Serbetli, S. and A. Yener, 2004. Time-slotted multiuser MIMO systems: Beamforming and scheduling strategies. *EURASIP. J. Wireless Commun. Networking*, 2004: 286-296.
- Shrivastava, N. and A. Trivedi, 2015. Combined beamforming with space-time-frequency coding for MIMO-OFDM systems. *AEU. Intl. J. Electron. Commun.*, 69: 878-883.
- Wang, W.Q., 2013. Phased-MIMO radar with frequency diversity for range-dependent beamforming. *IEEE. Sens. J.*, 13: 1320-1328.
- Yang, Y. and H. Yue, 2015. Efficient beamforming method for downlink MU-MIMO broadcast channels. *AEU. Intl. J. Electron. Commun.*, 69: 636-643.